JOURNAL OF MATERIALS SCIENCE 19 (1984) 567–573

Hydrogen effects on phase transformations in austenitic stainless steels

P. ROZENAK*, L. ZEVIN*†, D. ELIEZER*
*Materials Engineering Department and †Applied Research Institute, Ben-Gurion University of the Negev, Beer Sheva, Israel

The effects of hydrogen and stress (strain) on the phase transitions of a variety of stainless steels (316, 321, 347) were investigated. Hydrogen was introduced by severe cathodic charging at room temperature. X-ray diffraction was employed to reveal the transformations occurring in thin surface layers. After charging expanded ϵ phase is always present. α' martensite content increases during ageing and the final content depends on the stability of the austenite. The broadening of diffraction peaks of austenite after cathodic charging is caused by nonuniform distribution of hydrogen. The state of hydrogen distribution in the steel and the relationship between internal stresses, surface cracking and phase transition is discussed.

1. Introduction

An austenitic stainless steel such as an Fe–Ni–Cr is known to transform into ϵ (h c p) and α' (b c c) martensites during plastic deformation below the M_d temperatures (where M_d is the temperature at which 50% austenite has transformed to martensite during a tensile test at a true strain of 0.3). Because of the formation of the two types of martensites there has been a great deal of argument concerning the transformation sequence, i.e. whether the α' martensite form directly from the γ (f c c) phase or not. A detailed review and discussions on this is given by Nishiyama [1].

Hydrogen induced martensite phase transformation in austenite stainless steels have been extensively studied with respect to the relative stability of the austenitic phase. The effect of hydrogen on the γ-phase stability is that hydrogen decreases the γ-phase stability and may induce transformation of the γ phase to α' and/or ϵ martensite [2–8]. While austenite instability resulting from cathodic charging is generally agreed upon, the nature of the different phases, the sequence in which they appear and the kinetics of the processes are not well established. An understanding of the influence of hydrogen on the stability of austenite relative to a martensitic transformation is basic to an understanding of the mechanism of hydrogen embrittlement, and in view of the apparent contradiction in the available evidence, attempts to clarify this issue has been made by observations of hydrogen induced transformation in 316, 321 and 347 austenitic stainless steels.

In the present study we will examine the effects of hydrogen and the internal stresses on the phase transitions of a variety of stainless steels (316, 321, 347). The state of hydrogen distribution in the steel and the relationship between internal stresses, surface cracking and phase transition is discussed.

2. Experimental procedure

The studies were carried out on 316, 321 and 347 type austenitic stainless steels. The steels were of commercial grade, of composition shown in Table I, and were received in the form of sheets 0.1 mm thick. All of the samples used in these experiments were solution annealed for 1 h at 1100° C and then water quenched. Two austenitic grain sizes, ASTM-11 for 316 and ASTM-13 for 321 and 347 type stainless steels were obtained by varying austenizing time. The hydrogen charging was performed at room temperature in 1 N H_2SO_4 solution with 0.25 g l^{-1} of $NaAsO_2$ added as a hydrogen recombination poison. A platinum counter electrode and a current density of 50 mA

0022–2461/84 $03.00 + .12

TABLE I Chemical composition of types 316, 321 and 347 austenitic stainless steels (element in wt %)

	316	321	347
Cr	17.98	18.07	17.90
Ni	12.09	10.11	9.09
Mn	1.71	1.32	1.51
Si	0.879	1.033	1.025
C	0.05	0.072	0.064
Mo	2.08	–	–
Ti	–	0.41	–
Nb	–	–	0.61

cm^{-2} were used. A conventional Philips diffractometer equipped with step-motor, programmer, and teletype printer was used for X-ray diffraction study. The choice of the X-ray wavelength is of special importance: in diffractions with reflection (Bragg–Brentano) geometry, only information from the thin surface layer of the flat sample is obtained. The intensity I_t of rays scattered by the surface layer of thickness t is equal to [9]:

$$I_t/I_\infty = 1 - \exp[-2\mu t/(\sin\theta)] \quad (1)$$

where I_∞ is the intensity of rays scattered by an infinitely thick sample, μ is the linear absorption coefficient of the material, and θ is the Bragg angle.

The thickness to $t_{0,95}$, representing 95% of the total intensity of scattered rays, may be calculated from Equation 1 for various diffraction peaks and radiations. For the 111 austenite peak and radiations Cu$K\alpha$, Co$K\alpha$, Cr$K\alpha$, and Mo$K\alpha$ a value of $t_{0,95}$ equal to 2.6, 6.2, 8.7 and 8.7 μm, respectively, was obtained. As was reported elsewhere [10] cracks produced by severe cathodic charging propagate inside the material to a depth approximately equal to the grain size (8 to 10 μm). It is essential to characterize this damaged layer. It is evident that the Cu$K\alpha$ radiation is inappropriate. Among other radiations, Co$K\alpha$ radiation reveals the best combination of high intensity, angular resolution, and satisfactory depth of penetration, and therefore, it was used for most of the diffraction examinations, except quantitative phase analysis of thin surface layers. The latter was performed according to a special method using various radiations (Cu$K\alpha$, Co$K\alpha$, Cr$K\alpha$ and Mo$K\alpha$) and intensity measurements of various diffraction peaks [11].

3. Results

X-ray diffraction results obtained after hydrogen charging are presented in Table II. The diffraction patterns of the 316, 321, 347 types austenitic stainless steels reveals the presence of α'(b c c) that is formed after plastic deformation at room temperature. After cathodic charging and after tensile tested while undergoing cathodic charging, both α' and ϵ martensites were detected.

Induced phase transitions by cathodic charging of hydrogen into austenitic stainless steels is also observed by others [8, 10, 12]. X-ray diffraction patterns of 316 type taken after various times of charging and ageing are shown in Fig. 1. Diffraction peaks shift, lines broaden, and the appearance of new reflections were observed after hydrogen charging and during outgassing after charging. The diffraction lines of martensitic phase are detectable for 316, 321 and 347 types, the intensity is increased by 2 h ageing time (Fig. 2). For the more stable 316 type, the α' phase appears only after prolonged ageing of 24 h (Fig. 1). The fraction of martensitic phase increases with time of charging, corresponding to austenite decreases (Fig. 1). Hydrogen penetration considerably expands the lattice of both austenitic and martensitic phases and causes the greater shift of diffraction peaks toward the lower 2θ angles. The shift increases with charging time. For 316 type steel after 24 h of charging the centroid of the 111 peak is displaced by 1.15 of 2θ angle. This displacement corresponds to the lattice expansion ~2%. The second interesting effect of hydrogen penetration is peak broadening of the γ and ϵ-phases, which also increases with time of charging. On diffractograms taken after 5 min of ageing, splitting of $\gamma:\gamma^*$ and $\epsilon:\epsilon^*$ diffraction peaks was observed. After ageing the split peaks reformed into two singlets and shifted to the regular position of the uncharged samples. This shift of austenitic peaks is accompanied by decreasing peak width and after ageing for 288 h, the peak width is approximately the same as for the uncharged sample. However, the peak broadening of ϵ-martensite decreases with ageing time, but persists even after prolonged ageing of 288 h.

The distribution of the retained ϵ-martensite in the surface layer of the 321 type steel is shown on Fig. 3. The sample was charged for 24 h and measurements were undertaken from austenitic stabilized phases after 72 h of ageing. The fraction of ϵ-martensite drops from 70 to 80% on the surface to zero at the depth of approximately 5 μm. Surface deformation after cathodic charging has been observed indicating the development of high

TABLE II d-spacing of 316, 321 and 347 stainless steel, as received, tensile tested, cathodic charged and tensile tested undergoing cathodic charging

Phase	316 SS (observed)				321 SS (observed)				347 SS (observed)				Reported in literature (Holzworth and Louthan [12])		
	as received	tensile tested	cathodic charged*	tensile tested while undergoing cathodic charging*	as received	tensile tested	cathodic charged*	tensile tested while undergoing cathodic charging*	as received	tensile tested	cathodic charged*	tensile tested while undergoing cathodic charging*	ϵ-Martensite (L.B. Pfeil)	γ-Fe	α-Fe
$\epsilon_{(01.0)}$	–	–	–	2.187	–	–	2.179	2.164	–	–	2.173	2.173	2.199	–	–
$\epsilon_{(00.2)}$, $\gamma_{(111)}$	2.058	2.052	2.056	2.052	2.050	2.048	2.052	2.056	2.052	2.056	2.056	2.052	2.073	2.08	–
$\alpha'_{(110)}$	–	2.029	2.030	2.032	–	2.032	2.034	2.029	–	2.036	2.013	2.030	–	–	2.0268
$\epsilon_{(01.1)}$	–	–	1.932	1.932	–	–	1.922	1.920	–	–	1.922	1.969	1.942	–	–
$\gamma_{(200)}$	1.784	1.781	1.783	1.782	1.781	1.781	1.780	1.775	1.798	1.783	1.779	1.775	–	1.80	–
$\epsilon_{(01.2)}$	–	–	1.479	–	–	–	1.485	1.504	–	–	1.487	–	1.508	–	–
$\alpha'_{(200)}$	–	–	–	–	–	–	–	1.432	–	–	1.429	–	–	–	1.4332
$\epsilon_{(11.0)}$, $\gamma_{(220)}$	1.267	1.264	1.266	1.269	1.262	1.262	1.266	1.263	1.263	1.262	1.263	1.263	1.269	1.27	–
$\alpha'_{(211)}$, $\epsilon_{(013)}$	–	–	1.191	–	–	–	1.191	1.165	–	1.167	1.160	1.166	1.170	–	1.1702
$\epsilon_{(02.0)}$	–	–	–	–	–	–	–	–	–	–	–	–	1.099	–	–
$\epsilon_{(11.2)}$, $\gamma_{(311)}$	1.082	1.081	1.081	1.081	1.079	1.078	1.080	1.078	1.080	1.086	1.080	1.079	1.082	1.083	–
$\epsilon_{(02.1)}$	–	–	–	–	–	–	–	–	–	–	–	–	1.062	–	–
$\epsilon_{(004)}$, $\gamma_{(222)}$	1.035	1.035	1.035	1.036	–	–	–	–	–	–	1.033	1.036	1.036	1.037	–
$\alpha'_{(220)}$	–	–	–	–	–	–	–	–	–	–	–	–	–	–	1.0134
$\alpha'_{(310)}$	–	–	–	–	–	–	–	–	–	–	–	–	–	–	0.9064

*XRD analysis was performed after the ageing for one week.

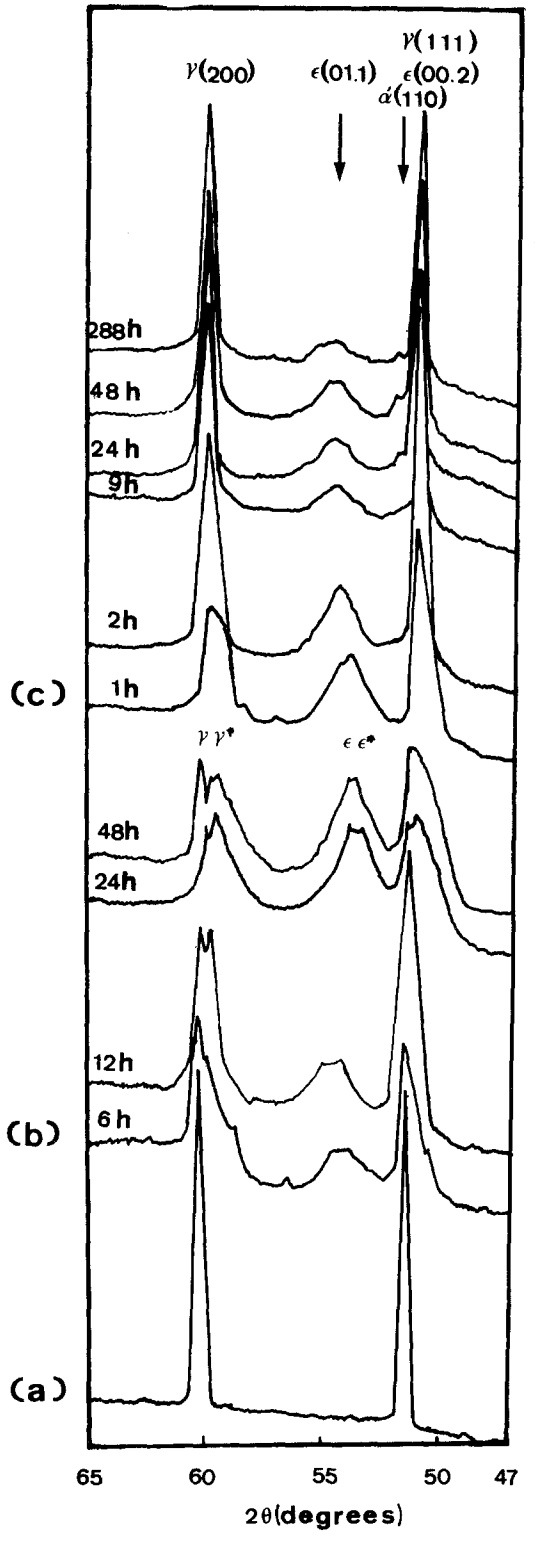

Figure 1 X-ray diffraction patterns of 316 stainless steel: (a) uncharged, (b) after cathodic charging of 6, 12, 24 and 48 h (diffractograms were taken immediately after charging), and (c) after ageing times of 1, 2, 9, 48 and 288 h (originally 48 h cathodically charged).

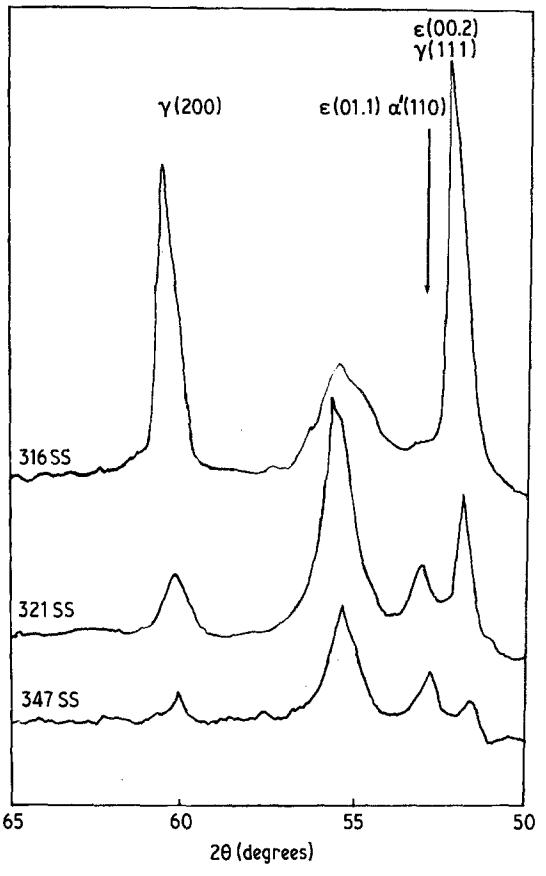

Figure 2 X-ray diffraction patterns of 316, 321 and 347 stainless steels after ageing of 2 h (48 h cathodic charged).

tensile surface stresses [10]. Scanning electron micrographs of the surface cracking of 316 type steel after charging for 24 h are given in Fig. 4. The cross section micrograph taken after 24 h of charging reveals that the cracks extended to a depth of about 10 μm.

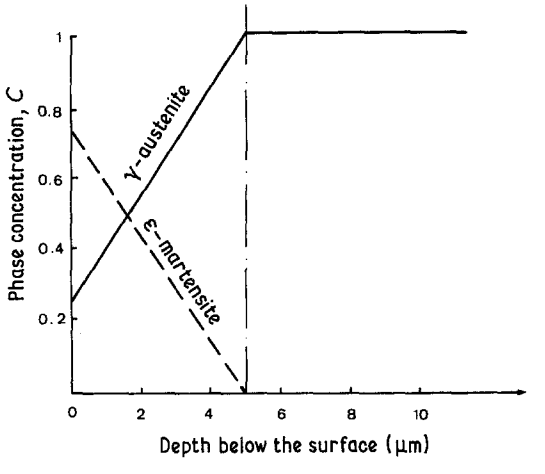

Figure 3 Phase distribution in surface layer in 321 stainless steel cathodically charged.

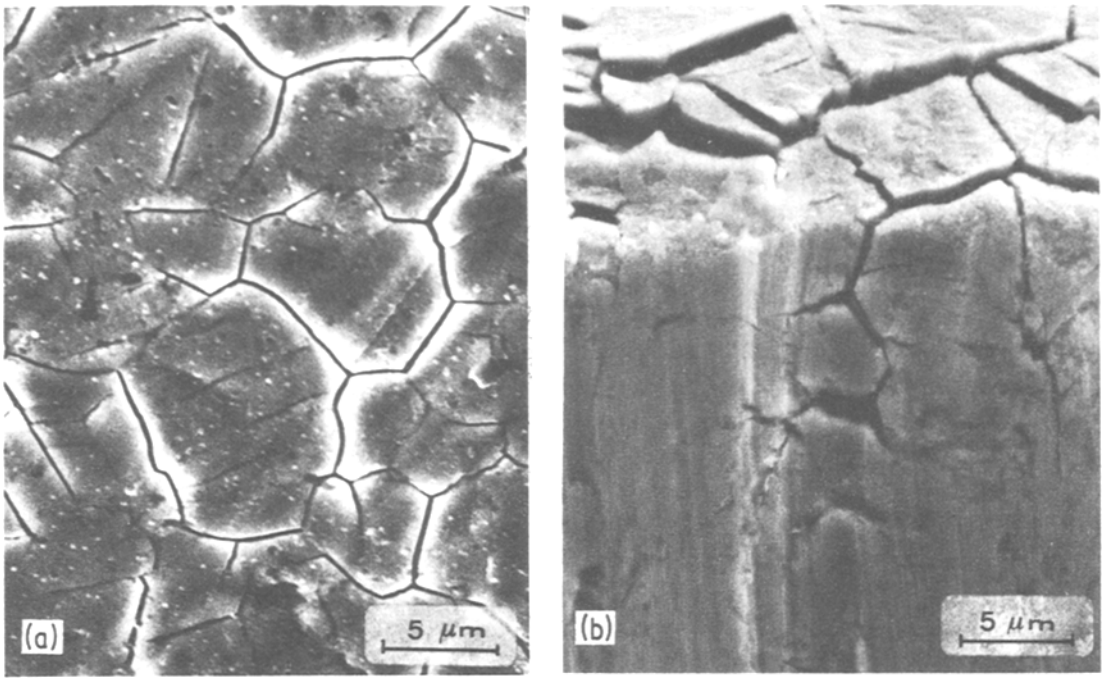

Figure 4 Scanning electron micrographs of surface cracks formed in unstressed 316 type specimens: (a) after 24 h of cathodic charging, and (b) cross-section of the same specimen.

4. Discussion

The stability of the austenite in Fe–Ni–Cr stainless steels is affected by solute H and stress. In order that the observed phase transitions and their relation to hydrogen effects in stainless steels be understood, the effects of stress as well as the effects of hydrogen concentration and distribution must be considered. In the uniform solid solution, the intensity of the diffraction peaks decreases due to local lattice distortion, but the peaks themselves remain sharp. The reason for peak broadening (Fig. 1) is the formation of nonuniform solid solution of hydrogen in austenite. Since both hydrogen penetration during charging and hydrogen release during ageing are diffusion controlled, their large concentration gradients in the thin surface layer (comparable with the depth of X-ray penetration) are expected. A schematic diagram of the relative concentrations of hydrogen after charging and after ageing is shown in Fig. 5.

During the ageing process hydrogen loss is expected primarily through the external surface. The hydrogen concentration during ageing is quickly reduced to low values at the surface, reaches a peak just below the surface, and then decreases at greater depths [8]. Actually, the hydrogen concentration is nonuniform within a single grain and this nonuniform concentration of hydrogen results in nonuniform expansion, which leads to the development of the internal stresses. The following models are considered in order to estimate the magnitude of the stresses.

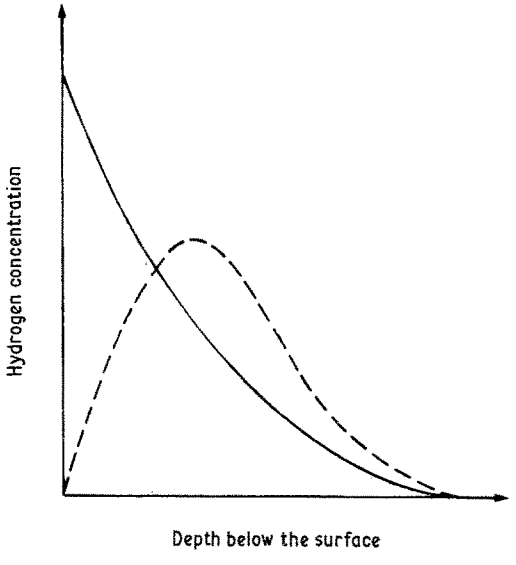

Figure 5 Schematic illustration of hydrogen concentration in the specimen during charging (full line) and after ageing (dashed line).

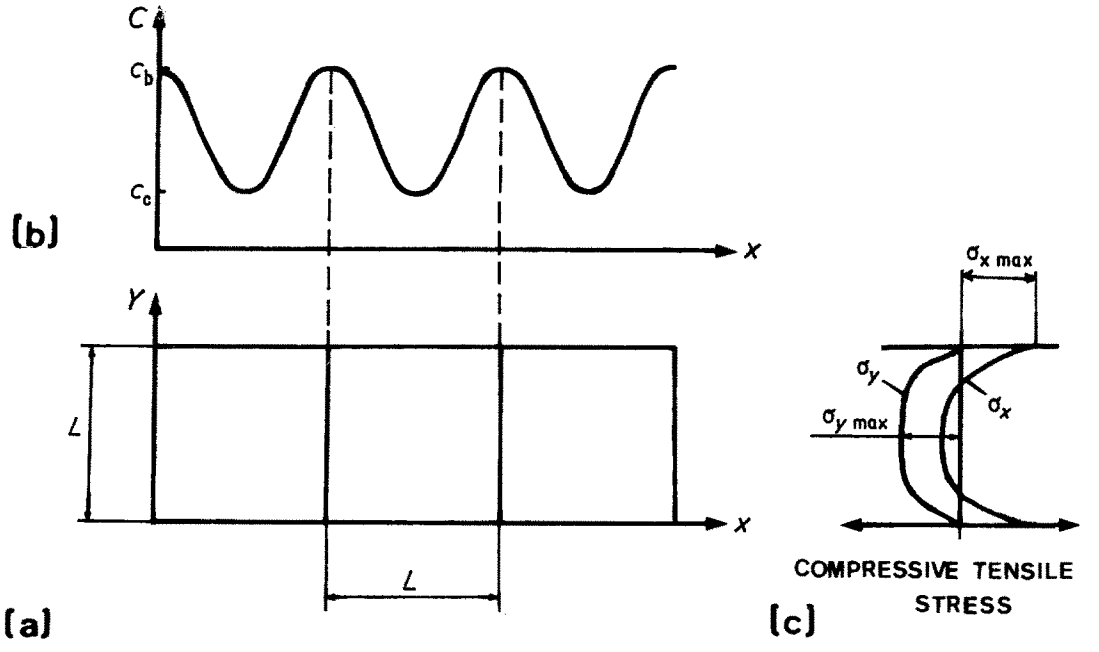

Figure 6 Schematic illustration of a one grain model with a hydrogen concentration profile (charging process). C_b and C_c – maximal and minimal concentration of hydrogen.

4.1. One-grain model

As was shown elsewhere [10], intergranular diffusion of hydrogen is much faster than transgranular diffusions. As a first approximation, a grain may be regarded as a sphere of radius b with hydrogen concentration increasing from the surface of the sphere to the centre during charging and in opposite direction during ageing (Fig. 6). In the one-grain model, tensile stresses are developed in the centre of the grain during charging and compressive stresses during ageing.

4.2. The multigrain model

This model takes into account the interaction between grains. The sample is represented by a two-dimensional sheet of similar rectangular grains of width L (Fig. 7a). The distribution of hydrogen concentration is periodical (Fig. 7b). The maximum of the concentration corresponds either to the grain boundary (charging process) or to the centre of the grains (ageing process). The schematic distribution of stresses during charging for this model is shown in Fig. 7c; tensile stresses σ_x are developed in the boundary areas. The stresses were calculated according to the theory of thermoelastic strains [14]. The maximum strain was estimated from the width of the 1 1 1 (austenite) peak ($\sim 3^\circ$ of the 2θ angle). The stresses calculated for the sample charged for 24 h were of the order of 5×10^9 Pa for both the proposed models [11], i.e. well above the ultimate tensile stress for 316 stainless steel. As the internal stresses would be expected to increase with charging time than stress relaxation should occur; evidence of such relax-

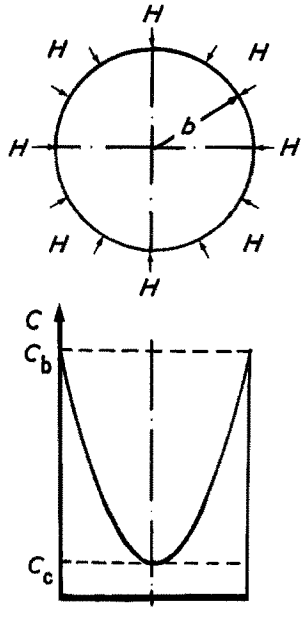

Figure 7 Schematic illustration of multigrain model: (a) geometrical model, (b) distribution of hydrogen concentration in charging process, and (c) distribution of stresses along grain boundary in charged process.

ation is shown by crack formation (Fig. 4). The crack network indicates that the material was broken into small subgrain blocks; it is probably that the distribution of hydrogen within a single block is uniform. The distribution of hydrogen in the entire material, remains nonuniform and retains the features mentioned earlier. The distribution curves calculated by Atrens *et al.* [15] on the basis of a planar diffusion model, shown schematically in Fig. 5 may be regarded as the first approximation. Because of intergranular diffusion of hydrogen and crack formation the real distribution is probably not smooth but stepped. The second phenomena induced by internal stresses is phase transition of austenite to ϵ and α' martensite. This transition is promoted by decreasing the stacking fault energy of the austenite [5, 12, 13, 16]. The formation of plates of ϵ-phase and plate-like highly faulted areas of austenite is described elsewhere [5]. It is proposed that the formation of ϵ-martensite is the result of accumulation of stacking faults in the austenite. This phenomenon as well as the thinness of the ϵ-phase plates is the reason of retained broadening of ϵ-peaks after prolonged ageing. The ϵ-phase is generated in the thin ($\sim 5\,\mu$m) surface layer of the samples (Fig. 3). This layer is characterized by a gradient of hydrogen concentration [15] and the development of high tensile surface stresses. Narita *et al.* [8] have suggested that the stainless steel–H system appears to have a miscibility gap in which the γ phase, containing about 21% H, is in equilibrium with the γ^* phase, containing about 55% H. From the work reported here, the appearance of γ and γ^* as well as ϵ and ϵ^* is a result of a very special hydrogen distribution. This issue will be discussed in detail elsewhere [17].

5. Conclusions

1. X-ray diffraction reveals that after charging of 6, 12, 24 and 48 h, an expanded ϵ martensite phase is always present. α' martensite content increases during ageing after charging and the final content depends on the stability of the austenite.

2. The broadening of the diffraction peaks, of austenite after cathodic charging is due to nonuniform distribution of hydrogen.

3. Nonuniform expansion and contraction of the steel during charging and ageing process leads to development of internal stresses.

4. 321 and 347 type austenitic stainless steels respond in a different way to type 316 austenite stainless steel during hydrogen charging.

References

1. Z. NISHIYAMA, "Martensitic Transformation", edited by M. E. Fine, M. Meshii and C. M. Wayman (Academic Press, London, 1978) p. 60.
2. M. L. HOLZWORTH, *Corrosion* 25 (1969) 107.
3. C. L. BRIANT, *Met. Trans.* 9A (1978) 731.
4. D. ELIEZER, D. G. CHAKRAPANI, C. J. ALTSTETTER and E. N. PUGH, *ibid.* 10A (1979) 935.
5. E. MINKOVITZ, M. TALIANKER and D. ELIEZER, *J. Mater. Sci.* 16 (1981) 2507.
6. E. MINKOVITZ and D. ELIEZER, *J. Mater. Sci. Lett.* 1 (1982) 192.
7. N. NARITA and H. K. BIRNBAUM, *Scripta Metall.* 14 (1980) 1355.
8. N. NARITA, C. J. ALTSTETTER and H. K. BIRNBAUM, *Met. Trans.* 13A (1982) 1355.
9. H. P. KLUG and L. E. ALEXANDER, "X-Ray Diffraction" (John Wiley, New York, 1974) p. 360.
10. P. ROZENAK, L. ZEVIN and D. ELIEZER, *J. Mater. Sci. Lett.* 2 (1983) 63.
11. P. ROZENAK and L. ZEVIN and D. ELIEZER, *J. Appl. Cryst.* in press.
12. M. HOLZWORTH and M. LOUTHAN Jr, *Corrosion* 24 (1968) 110.
13. K. KAMACHI, M. OKA and M. TOUGE, "New Aspects of Martensitic Transformation", (Japan Institute of Metals Sendai, 1976) p. 309.
14. S. P. TIMOSHENKO and J. N. GOODIER, "Theory of Elasticity" (McGraw Hill, New York, 1970) p. 433.
15. A. ATRENS, J. J. BELLINA, N. F. FIORE and R. J. COYLE, Proceedings of the Symposium on the Metals Physics of Stainless Steels (TMS-AIME, Denver, Colorado, 1978) p. 54.
16. P. MAULIK and J. BURKE, *Scripta Metall.* 9 (1975) 17.
17. P. ROZENAK, L. ZEVIN and D. ELIEZER, to be published.

Received 14 February
and accepted 15 June 1983